


Impact of Compositional Nonuniformity in (In,Ga)N-Based Light-Emitting Diodes

A. Di Vito,¹ A. Pecchia,² A. Di Carlo,¹ and M. Auf der Maur^{1,*}

¹*Department of Electronics Engineering, University of Rome Tor Vergata, Via del Politecnico 1, 00133 Rome, Italy*

²*CNR-ISMN, Via Salaria Km 29.300, 00017 Monterotondo (Rome), Italy*

 (Received 10 December 2018; revised manuscript received 12 May 2019; published 29 July 2019)

Carrier localization due to statistical fluctuations in indium gallium nitride alloys has been recognized to play an important role for the performance of light-emitting diodes, both experimentally and through theoretical studies. While a random-alloy assumption is usually made, in this work we take into account the presence of spatial nonuniformities in the indium content on the nanometer scale and we theoretically analyze their impact on the electronic and optical properties of the alloy and the device. We show that indium clustering induces tail states in both the conduction and valence bands. This causes a reduction of the band gap and a broadening of the optical absorption edge. Furthermore, compositional fluctuations in the active region of the device determine a substantial broadening of the optical emission spectrum and a decrease of the peak emission energy, in agreement with experimental results. Moreover, the radiative recombination coefficient increases for an increasing degree of clustering, suggesting a transition to a quantum-dot-like structure. Finally, the temperature dependence of the radiative coefficient derived for the nonuniform structures is in good agreement with the experimental results, which show a temperature behavior opposite to the trend expected from standard theoretical considerations.

DOI: [10.1103/PhysRevApplied.12.014055](https://doi.org/10.1103/PhysRevApplied.12.014055)

I. INTRODUCTION

Indium gallium nitride is a successful material for the realization of efficient short-wavelength commercial light-emitting diodes (LEDs) [1–3]. In fact, (In,Ga)N potentially covers the whole visible spectrum—thus, in principle, allowing elimination of phosphor-based down-conversion and enabling a color-mixing approach, which would allow the overall white-LED efficiency to be further increased [4].

Although the technology for (In,Ga)N-based blue and white LEDs has been successfully commercialized, there are several material-related issues, such as efficiency droop, the green gap, compositional nonuniformity, and the spatial localization of carriers, which are still subject to debate [5–11]. While structural characterization reveals a compositional uniformity compatible with the assumption of a random alloy in high-quality structures [12], one should expect some deviation from such an idealized structure on the atomic scale. Previous studies show that the fluctuations in the local indium concentration, even in the case of a uniform random alloy, lead to the breaking of translational symmetry and spatial localization of carriers [13–18]. Interestingly, the hole localization, which is particularly evident in samples containing indium clusters,

appears to have a strong influence on the alloy properties [19,20].

In most of the studies conducted so far, the impact of deviations from a uniform random alloy on the properties of (In,Ga)N has not been discussed [7,8,13,14,21,22]. Furthermore, the theoretical analysis based on density-functional theory (DFT) performed on clustered (In,Ga)N bulk structures [23,24] lacks an appropriately large supercell size and a sufficiently large number of random samples. Thus, a discussion of the role of clustering for the properties of (In,Ga)N alloys and the performance of (In,Ga)N-based LEDs, supported by a proper statistical characterization of the samples, is still needed.

In the present work, we theoretically describe the optical properties of bulk (In,Ga)N alloys and (In,Ga)N/GaN single-quantum-well (SQW) LEDs, taking into account the statistical fluctuation of the alloy composition and the presence of indium clusters. In particular, we study the transition from a perfect random alloy toward a nonuniform one. In Sec. II, we present the theoretical approach used to perform the simulations and we describe in detail the method employed to generate the samples, with several amounts of nonuniformity. The results of the simulations are shown in Secs. III A and III B for the bulk material and the device, respectively. We analyze the outcomes of our study and compare them with the experimental measurements, in terms of the energy gap, the optical-absorption coefficient,

*auf.der.maur@ing.uniroma2.it

the emission spectra, and the temperature dependence of the radiative coefficient. We discuss the influence of compositional nonuniformity on the optical properties of both the bulk alloy and the device.

II. THEORETICAL APPROACH

In order to theoretically study the effect of alloy nonuniformity on the performance of macroscopic devices, we use a computational scheme combining continuum and atomistic models. To obtain the electronic and optical properties of both the bulk material and the device, we use an atomistic empirical-tight-binding (ETB) approach [25,26]. The atomistic structures are first relaxed using a Keating valence-force-field (VFF) method [27]. The parameters α and β of the model are computed to reproduce the bulk elasticity tensor of the pure materials. In the random alloy, for each In—N and Ga—N bond, we use the corresponding bulk values for α and β . Then, we compute the electron and hole states, from which we calculate the momentum-matrix elements (MMEs), the optical spectra, and the density of states (DOS).

For the simulations of the bulk material, we compute the first 12 electron and 24 hole states at the Γ point of the Brillouin zone. We use $10 \times 10 \times 10 \text{ nm}^3$ periodic supercells with a mean indium content of $x = 20\%$, corresponding to a value lying in between those needed to obtain blue and green quantum-well LEDs. The qualitative results and trends demonstrated in this study, however, are valid for the whole range of technologically relevant indium-content values.

The random-alloy samples are generated by substituting gallium atoms with indium atoms at random, assuming a spatially uniform substitution probability equal to the mean indium concentration. Differently, for the nonuniform alloy we first distribute uniformly a certain percentage of the indium atoms, which we denote in the following as the percentage of uniformity in order to identify different structures. The remaining indium atoms are then distributed with a spatially varying probability as follows. We first pick a gallium atom at random. Then we count the indium atoms around this gallium up to the second-nearest cation site and we calculate the substitution probability as the ratio of this number and the available cation sites, leading, therefore, to a spatial correlation. This is repeated until all necessary indium atoms are distributed. Note that the total number of indium atoms is always the same, in order to fix the mean indium content.

The degree of clustering can be controlled by the percentage of uniformly distributed indium atoms, for which we use values of 100% (random alloy), 80%, 60%, and 40% of the total number of indium atoms. The lower the percentage, the more clustering can be expected. To obtain statistically significant results, we simulate 50 structures for the uniform random-alloy configuration, as well as for

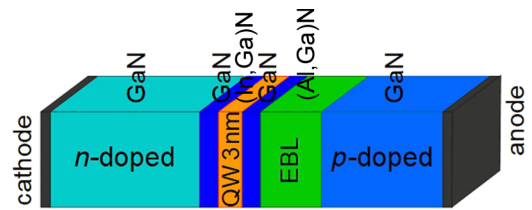


FIG. 1. A schematic view of the simulated structure.

the slightly clustered alloy (80% uniformity). For the other cases, we use 100 random samples, since the statistical variations are more pronounced for the strongly clustered samples.

For the (In,Ga)N/GaN SQW LED, we use a structure as shown schematically in Fig. 1, assuming a mean indium content of $x = 20\%$ and a well width of 3 nm. The considered device has the same structural parameters as those used for the calculations performed by Auf der Maur *et al.* [7]. In fact, the present work can be regarded as an extension of the mentioned study, in which the nonuniformity of the (In,Ga)N alloy was not addressed. Although spatial variations of the QW thickness can be expected in real LEDs, and they influence the device behavior as shown, e.g., in Refs. [22] and [28], here we assume ideal QW interfaces in order to not mix different effects in our study. However, well-width variations could be taken into account in our simulation model, using an approach similar to that in the analysis of Tanner *et al.* [22].

All simulations have been performed for a LED operating point close to the maximum internal quantum efficiency and a periodic supercell of $10 \times 10 \text{ nm}^2$ is chosen in the quantum-well plane. To obtain the electrostatic potential, which is needed to set up the tight-binding Hamiltonian, and the quasi-Fermi levels at the chosen operating point, we first solve the one-dimensional (1D) Schrödinger–drift–diffusion problem, using the TIBERCAD software [29]. The potential is then projected onto the atomic positions, thus neglecting variations in the QW plane. For the calculation of the optical spectra, we compute the first eight electron and 12 hole states in the Γ , M , X , and Y points of the reduced Brillouin zone and we use the trapezoidal method for reciprocal space integration.

III. RESULTS AND DISCUSSION

In this section, we show the results of the simulations performed for the $\text{In}_{0.2}\text{Ga}_{0.8}\text{N}$ alloy (Sec. III A) and the $\text{In}_{0.2}\text{Ga}_{0.8}\text{N}/\text{GaN}$ SQW LED (Sec. III B), where the fluctuations of the indium content are taken into account. We analyze the outcomes of our theoretical derivation and discuss the comparison with the experimental measurements. We demonstrate that it is crucial to consider the presence of compositional nonuniformity in order to properly describe

the optical properties of both the bulk material and the device.

A. Bulk $\text{In}_{0.2}\text{Ga}_{0.8}\text{N}$ alloy

In Fig. 2, we show the mean DOS, i.e., the weighted sum of the DOS values of all random samples. We can clearly see that indium clustering yields tail states both in the conduction and the valence bands and reduces the band gap by approximately 0.5 eV compared to the uniform alloy, confirming the results reported in previous studies [24,30–32]. Moreover, the band-gap values calculated taking into account the nonuniformities of the samples are in reasonable agreement with the experimental data found in the literature [33–35], as reported in Table I for completeness. Note that for the random-alloy case, only an insignificant broadening of the band edges is predicted. These band tails are due to the strong scattering in the energies of the electron and hole ground states, which increases with increasing deviation from a uniform alloy. This effect is associated with increasing localization of the carrier wave functions, which is correlated with the degree of indium clustering [36].

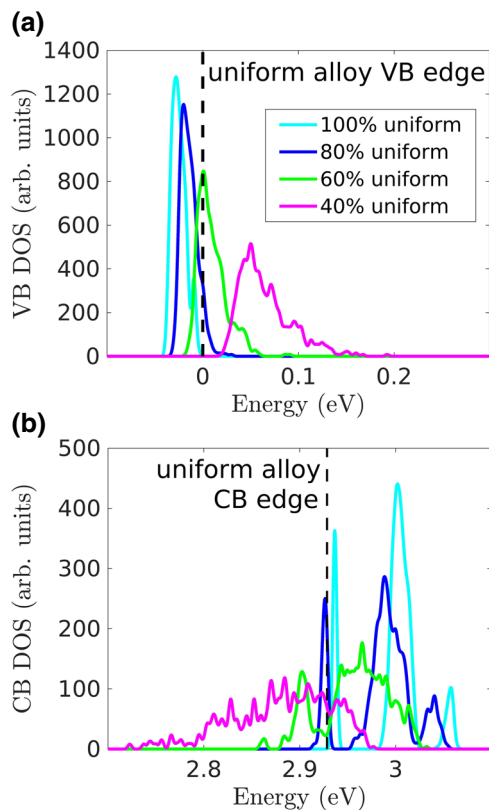


FIG. 2. The DOS (sample average) for a bulk $\text{In}_{0.2}\text{Ga}_{0.8}\text{N}$ alloy with several different percentages of uniformly distributed indium atoms, resulting in several degrees of clustering. The valence and conduction band states are represented in (a) and (b), respectively.

TABLE I. The calculated and measured energy-gap values. The theoretical results are reported for the uniform alloy and the structure with the highest degree of clustering. The experimental values 1, 2, and 3 refer to the studies of Wu *et al.* [33] (absorption measurements), Moret *et al.* [35], and Franssen *et al.* [34] (PL measurements), respectively.

	Energy gap (eV)
This work	$2.9 \xrightarrow{\text{clustering}} 2.5$
Experiment 1	2.7
Experiment 2	2.5
Experiment 3	2.4

Concerning the optical properties of the clustered bulk $\text{In}_{0.2}\text{Ga}_{0.8}\text{N}$ alloy, it is particularly interesting to analyze the behavior of the absorption spectrum, shown in Fig. 3. We observe an increasing broadening of the optical-absorption edge with an increasing degree of clustering and the washing out of a double-peak structure at the absorption edge. These trends are in good agreement with the experimental results reported by Butté *et al.* [37] on thick (In,Ga)N layers, at least under the reasonable assumption that a growing indium content leads to increased nonuniformity. Thus, the optical absorption edge broadening observed by Butté *et al.* could be explained by increasing nonuniformity in the indium distribution.

B. $\text{In}_{0.2}\text{Ga}_{0.8}\text{N}/\text{GaN}$ SQW LED

The mean emission spectra of the $\text{In}_{0.2}\text{Ga}_{0.8}\text{N}/\text{GaN}$ SQW LED are shown in Fig. 4 for each considered percentage of uniformly distributed indium atoms. The band-gap reduction, induced by the nonuniformity of the alloy composition, yields a red shift of the peak emission energy as the degree of indium clustering increases. Moreover, it can be seen that indium clustering induces a pronounced broadening of the spectrum. The measured

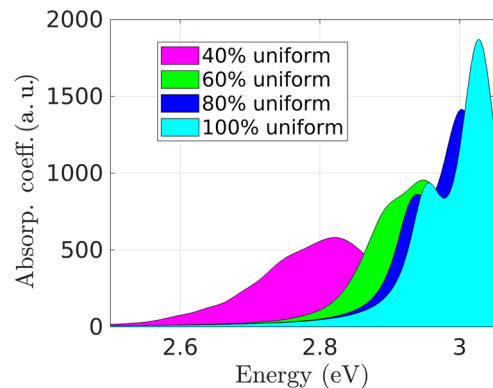


FIG. 3. The absorption coefficient (sample average) for a bulk $\text{In}_{0.2}\text{Ga}_{0.8}\text{N}$ alloy with several different percentages of uniformly distributed indium atoms, resulting in several degrees of clustering.

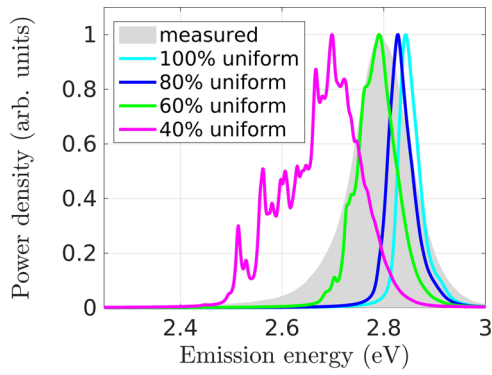


FIG. 4. The calculated emission spectra (sample average) for an $\text{In}_{0.2}\text{Ga}_{0.8}\text{N}$ quantum well at several different percentages of uniformity. The experimental spectrum [38] is depicted by the gray area.

emission spectrum of a SQW LED with a structure similar to the simulated one but a slightly lower indium content [38] is represented by the gray area in Fig. 4. Note that both the measured peak position and the spectrum width are better described by the model with a nonuniform alloy. In particular, the case of 60% uniformity seems to reproduce the experimental features rather well. The high-energy tail is well described, while the low-energy tail shows slightly too little broadening. Note that the 60% uniform samples are consistent with the atom-probe-tomography (APT) measurements reported in the literature [9,28] if the limited APT detection efficiency is taken into account [39]. This is discussed in detail in Sec. I of the Supplemental Material [36], where we analyze the indium distribution within the $\text{In}_{0.2}\text{Ga}_{0.8}\text{N}$ supercell for all the considered percentages of uniformity.

A scatter plot of the ground-state MMEs, evaluated at the Γ point of the Brillouin zone for all the simulated structures and for each percentage of uniformity, is shown

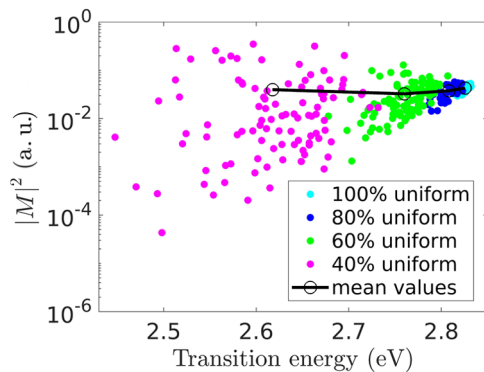


FIG. 5. The ground-state transition MME, i.e., the MME related to the optical transition from the electron ground state to the hole ground state, of an $\text{In}_{0.2}\text{Ga}_{0.8}\text{N}$ quantum well, calculated at the Γ point for several different percentages of uniformity. The results for each simulated sample are visualized as dots, while the sample average is labeled by black circles.

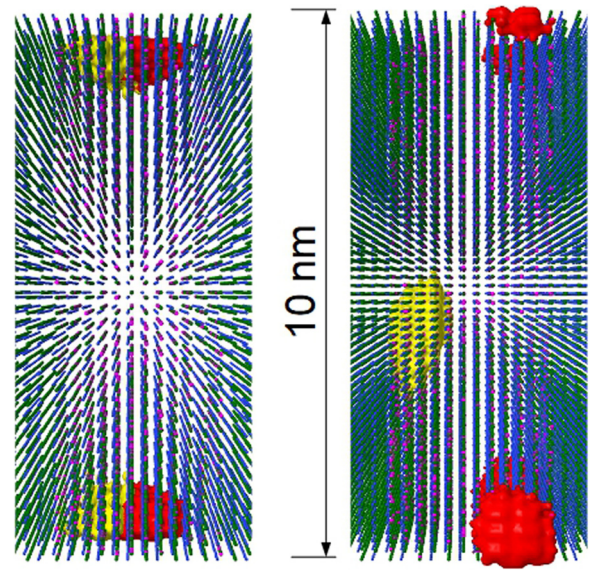


FIG. 6. The ground-state electron (red) and hole (yellow) wave functions for the $\text{In}_{0.2}\text{Ga}_{0.8}\text{N}$ quantum well with 40% (maximum clustering degree) of uniformly distributed indium atoms. Two structures are represented, corresponding to (right) the minimum and (left) the maximum value of the MME. The isosurfaces containing 50% of the total ground-state density are shown. Indium, gallium, and nitrogen atoms are depicted in magenta, green, and blue, respectively.

in Fig. 5. It can be seen that the increase in the degree of clustering causes an increasing spread in the calculated MME values. This behavior is due to the fact that the carrier localization induced by compositional fluctuations yields substantial statistical variations in the overlap of the electron and hole wave functions. This is illustrated in Fig. 6, where the ground-state electron and hole wave functions for the structures with the minimum and maximum MMEs are shown for the largest degree of clustering studied (40% of uniformity). Furthermore, we can see in Fig. 5 that the MME average value slightly decreases for small nonuniformity (up to 60% of uniformity) and then increases for the 40% uniform case. This is because, with substantial alloy nonuniformity, the indium clustering may localize both electrons and holes in the same spatial position, overcoming the quantum-confined Stark effect (QCSE), as is the case in the left panel of Fig. 6. Indeed, in such a case, the MME can be considerably larger than that of the random alloy. Otherwise, due to the QCSE, the electron and hole states are influenced by the largely independent indium-content fluctuations near the upper and lower QW interface, respectively [7].

The radiative recombination coefficient B for all the simulated structures and each considered percentage of uniformity is shown in Fig. 7. The B value for each structure is calculated assuming constant quasi-Fermi levels such that the mean carrier density is fixed and equal to $\bar{n} = \bar{p} = 5 \times 10^{11} \text{ cm}^{-2}$. The global radiative coefficient

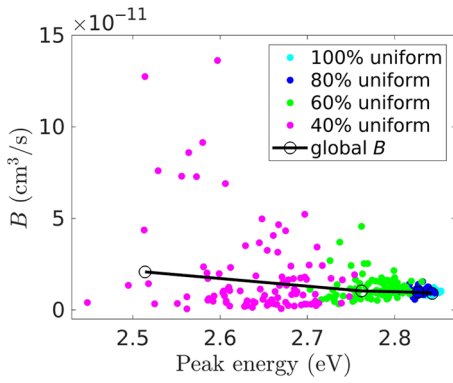


FIG. 7. The radiative recombination coefficient B of an $\text{In}_{0.2}\text{Ga}_{0.8}\text{N}$ quantum well for several different percentages of uniformity. The results for each simulated sample are visualized as dots and the global B is labeled by black circles.

is defined as $\bar{B} = \bar{R}_r / (\bar{n}\bar{p})$, where \bar{R}_r is the mean radiative recombination rate, i.e., the weighted sum of the radiative recombination rates of all random samples [7]. As expected from the behavior of the MME, the indium clustering induces an increment of the spread in the calculated values of B . However, while the mean ground-state transition MME decreases up to 60% of uniformity, the global value of the radiative coefficient increases for increasing nonuniformity. In fact, a higher number of optical transitions is allowed due to the breaking of the translational symmetry induced by the presence of disorder, as confirmed by the increase in the transition-related MME magnitude for an increasing degree of clustering [36]. Such an effect causes an increment of the radiative coefficient value when the nonuniformity of the structure increases. We could interpret the increase of the global B as the onset of the transition from QW to quantum-dot-like behavior, induced by the high degree of clustering, as suggested by the wave-function localization depicted in Fig. 6.

Finally, in order to obtain the temperature behavior of the radiative coefficient, we derive the occupation of the states using several values of temperature and adjusting the quasi-Fermi levels so that the mean carrier density is fixed. The temperature dependence of the global B thus obtained is shown in Fig. 8 for several values of the mean carrier density. Only for the 100% uniform structure does the radiative coefficient \bar{B} decrease with increasing temperature for all the considered values of the mean carrier density. This is compatible with simple QW theory, which predicts that B will be proportional to the inverse of the temperature [40]. For increasing nonuniformity, the temperature dependence of \bar{B} becomes mostly constant or even increasing with temperature, in net contrast to the theory. In fact, when nonuniformities are considered, strongly localized states are present that are located deeply inside the energy gap of the 100% uniform samples, as we discuss in Sec. III A. The MMEs related to the low-energy optical

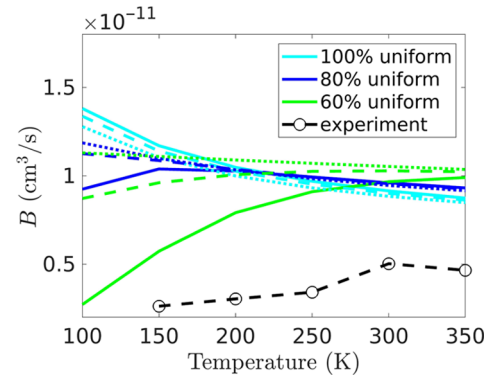


FIG. 8. The temperature dependence of B for an $\text{In}_{0.2}\text{Ga}_{0.8}\text{N}$ quantum well at several different percentages of uniformly distributed indium atoms. The solid, dashed, and dotted lines represent the values obtained for mean carrier densities of 10^{11} , 5×10^{11} , and 10^{12} cm^{-2} , respectively. Experimental data from Ref. [19] at a carrier density of approximately 10^{12} cm^{-2} are shown by black circles. The results for the 40% uniform structure are not reported in the figure, since their range of variation is too wide.

transitions between localized states of nonuniform structures have lower values with respect to the MMEs associated with higher-energy transitions, as shown in Fig. 1 of the Supplemental Material [36]. Thus, at low temperature, as the occupied states are mostly localized states, the radiative coefficient is lower with respect to the B value derived for higher temperatures, when the occupation of delocalized states becomes more important. Interestingly, this behavior better matches the measured data presented by Nippert *et al.* [19] for a blue multi-quantum-well LED, presumably having slightly lower indium content, and reported in the figure by black circles. In particular, the experimental trend is very similar to the behavior predicted for the 60% uniform structure with $\bar{n} = 5 \times 10^{11} \text{ cm}^{-2}$. Note that we are considering the temperature dependence of B and not its magnitude, which clearly differs from the experiment since the simulated device does not have exactly the same structural parameters as those of the LED analyzed by Nippert *et al.* [19], so that, in particular, the QCSE could be different.

IV. CONCLUSIONS

In conclusion, we consider the effect of small to moderate deviations from a random-alloy structure on the optical properties of bulk $\text{In}_{0.2}\text{Ga}_{0.8}\text{N}$ and a $\text{In}_{0.2}\text{Ga}_{0.8}\text{N}/\text{GaN}$ SQW LED. We find that, accounting for the nonuniformity of the alloy composition, band tails appear in the calculated DOS, inducing a reduction of the band-gap energy and a broadening of the optical absorption edge, in agreement with the experimental results. In turn, the decrease of the band gap yields a lower peak emission energy of the LED device, as the degree of clustering increases.

Furthermore, the indium content fluctuations determine a substantial broadening of the optical-emission spectrum of the LED. In fact, both the experimental peak energy and the width are better described when alloy nonuniformity is taken into account. Nevertheless, with our work we do not intend to rule out other mechanisms, such as excitonic effects, interface roughness [22,41,42], and built-in field and local field effects [16,43], which also lead to broadening and peak-emission reduction. Finally, when the presence of nonuniformity is considered, a higher number of optical transitions is allowed due to the breaking of the translational symmetry induced by clusters. This causes the radiative coefficient to increase for an increasing amount of clustering, suggesting a transition to a quantum-dot-like structure. We find that the experimental temperature dependence of the radiative coefficient can be well reproduced when assuming a nonuniform alloy. This is an interesting result, since the temperature behavior of B derived by standard theoretical considerations is opposite to the experimental trend.

ACKNOWLEDGMENT

This work has been supported by Horizon 2020 project ChipScope, under Grant Agreement No. 737089.

- [1] S. Nakamura, M. Senoh, and T. Mukai, P-GaN/N-InGaN/N-GaN double-heterostructure blue-light-emitting diodes, *Jpn. J. Appl. Phys.* **32**, L8 (1993).
- [2] S. Nakamura, in *Light-Emitting Diodes: Research, Manufacturing, and Applications* (International Society for Optics and Photonics, San Jose, 1997), Vol. 3002, p. 26.
- [3] H.-M. Kim, Y.-H. Cho, H. Lee, S. I. Kim, S. R. Ryu, D. Y. Kim, T. W. Kang, and K. S. Chung, High-brightness light emitting diodes using dislocation-free indium gallium nitride/gallium nitride multiquantum-well nanorod arrays, *Nano Lett.* **4**, 1059 (2004).
- [4] H. S. El-Ghoroury, M. Yeh, J. C. Chen, X. Li, and C.-L. Chuang, Growth of monolithic full-color GaN-based LED with intermediate carrier blocking layers, *AIP Adv.* **6**, 075316 (2016).
- [5] E. Taylor, P. R. Edwards, and R. W. Martin, Colorimetry and efficiency of white LEDs: Spectral width dependence, *Phys. Status Solidi (a)* **209**, 461 (2012).
- [6] J. Piprek, Efficiency droop in nitride-based light-emitting diodes, *Phys. Status Solidi (a)* **207**, 2217 (2010).
- [7] M. Auf der Maur, A. Pecchia, G. Penazzi, W. Rodrigues, and A. Di Carlo, Efficiency Drop in Green InGaN/GaN Light Emitting Diodes: The Role of Random Alloy Fluctuations, *Phys. Rev. Lett.* **116**, 027401 (2016).
- [8] C. M. Jones, C.-H. Teng, Q. Yan, P.-C. Ku, and E. Kioupakis, Impact of carrier localization on recombination in InGaN quantum wells and the efficiency of nitride light-emitting diodes: Insights from theory and numerical simulations, *Appl. Phys. Lett.* **111**, 113501 (2017).
- [9] M. J. Galtrey, R. A. Oliver, M. J. Kappers, C. J. Humphreys, D. J. Stokes, P. H. Clifton, and A. Cerezo, Three-dimensional atom probe studies of an $\text{In}_x\text{Ga}_{1-x}\text{N}/\text{GaN}$ multiple quantum well structure: Assessment of possible indium clustering, *Appl. Phys. Lett.* **90**, 061903 (2007).
- [10] M. J. Galtrey, R. A. Oliver, M. J. Kappers, C. J. Humphreys, P. H. Clifton, A. Cerezo, and G. D. W. Smith, Response to “Comment on Three-dimensional atom probe studies of an $\text{In}_x\text{Ga}_{1-x}\text{N}/\text{GaN}$ multiple quantum well structure: Assessment of possible indium clustering”, *Appl. Phys. Lett.* **91**, 176102 (2007).
- [11] J. A. Chan, J. Z. Liu, and A. Zunger, Bridging the gap between atomic microstructure and electronic properties of alloys: The case of (In,Ga)N, *Phys. Rev. B* **82**, 045112 (2010).
- [12] K. H. Baloch, A. C. Johnston-Peck, K. Kisslinger, E. A. Stach, and S. Gradečak, Revisiting the “In-clustering” question in InGaN through the use of aberration-corrected electron microscopy below the knock-on threshold, *Appl. Phys. Lett.* **102**, 191910 (2013).
- [13] T.-J. Yang, R. Shivaraman, J. S. Speck, and Y.-R. Wu, The influence of random indium alloy fluctuations in indium gallium nitride quantum wells on the device behavior, *J. Appl. Phys.* **116**, 113104 (2014).
- [14] M. López, A. Pecchia, M. Auf der Maur, F. Sacconi, G. Penazzi, and A. Di Carlo, Atomistic simulations of InGaN/GaN random alloy quantum well LEDs, *Phys. Status Solidi (c)* **11**, 632 (2014).
- [15] P. R. C. Kent and A. Zunger, Carrier localization and the origin of luminescence in cubic InGaN alloys, *Appl. Phys. Lett.* **79**, 1977 (2001).
- [16] M. A. Caro, S. Schulz, and E. P. O’Reilly, Theory of local electric polarization and its relation to internal strain: Impact on polarization potential and electronic properties of group-III nitrides, *Phys. Rev. B* **88**, 214103 (2013).
- [17] Z. Li, J. Kang, B. Wei Wang, H. Li, Y. Hsiang Weng, Y.-C. Lee, Z. Liu, X. Yi, Z. Chuan Feng, and G. Wang, Two distinct carrier localization in green light-emitting diodes with InGaN/GaN multiple quantum wells, *J. Appl. Phys.* **115**, 083112 (2014).
- [18] S. Schulz, M. A. Caro, C. Coughlan, and E. P. O’Reilly, Atomistic analysis of the impact of alloy and well-width fluctuations on the electronic and optical properties of InGaN/GaN quantum wells, *Phys. Rev. B* **91**, 035439 (2015).
- [19] F. Nippert, S. Y. Karpov, G. Callsen, B. Galler, T. Kure, C. Nenstiel, M. R. Wagner, M. Straßburg, H.-J. Lugauer, and A. Hoffmann, Temperature-dependent recombination coefficients in InGaN light-emitting diodes: Hole localization, Auger processes, and the green gap, *Appl. Phys. Lett.* **109**, 161103 (2016).
- [20] B. Lee and L. W. Wang, Band gap bowing and electron localization of $\text{Ga}_x\text{In}_{1-x}\text{N}$, *J. Appl. Phys.* **100**, 093717 (2006).
- [21] D. Oriato and A. B. Walker, Effects of piezoelectric field, bias and indium fluctuations on a InGaN—GaN single quantum well system, *Phys. B: Condens. Matter* **314**, 59 (2002), proceedings of the Twelfth International Conference on Nonequilibrium Carrier Dynamics in Semiconductors.

- [22] D. S. P. Tanner, J. M. McMahon, and S. Schulz, Interface Roughness, Carrier Localization, and Wave Function Overlap in c -Plane (In,Ga)N/GaN Quantum Wells: Interplay of Well Width, Alloy Microstructure, Structural Inhomogeneities, and Coulomb Effects, *Phys. Rev. Appl.* **10**, 034027 (2018).
- [23] X. Wu, E. J. Walter, A. M. Rappe, R. Car, and A. Selloni, Hybrid density functional calculations of the band gap of $\text{Ga}_x\text{In}_{1-x}\text{N}$, *Phys. Rev. B* **80**, 115201 (2009).
- [24] I. Gorczyca, S. P. Lepkowski, T. Suski, N. E. Christensen, and A. Svane, Influence of indium clustering on the band structure of semiconducting ternary and quaternary nitride alloys, *Phys. Rev. B* **80**, 075202 (2009).
- [25] J.-M. Jancu, R. Scholz, F. Beltram, and F. Bassani, Empirical spds* tight-binding calculation for cubic semiconductors: General method and material parameters, *Phys. Rev. B* **57**, 6493 (1998).
- [26] J.-M. Jancu, F. Bassani, F. D. Sala, and R. Scholz, Transferable tight-binding parametrization for the group-III nitrides, *Appl. Phys. Lett.* **81**, 4838 (2002).
- [27] D. Camacho and Y. Niquet, Application of Keating's valence force field model to non-ideal wurtzite materials, *Phys. E: Low-Dimension. Syst. Nanostruct.* **42**, 1361 (2010).
- [28] D. Watson-Parris, M. J. Godfrey, P. Dawson, R. A. Oliver, M. J. Galtrey, M. J. Kappers, and C. J. Humphreys, Carrier localization mechanisms in $\text{In}_x\text{Ga}_{1-x}\text{N}/\text{GaN}$ quantum wells, *Phys. Rev. B* **83**, 115321 (2011).
- [29] TIBERCAD simulation package, <http://www.tibercad.org>.
- [30] L. Bellaiche, T. Mattila, L.-W. Wang, S.-H. Wei, and A. Zunger, Resonant hole localization and anomalous optical bowing in InGaN alloys, *Appl. Phys. Lett.* **74**, 1842 (1999).
- [31] I. Gorczyca, T. Suski, N. E. Christensen, and A. Svane, Gap bowing in $\text{In}_x\text{Ga}_{1-x}\text{N}$ and $\text{In}_x\text{Al}_{1-x}\text{N}$ under pressure, *Phys. Status Solidi (c)* **6**, S368 (2009).
- [32] K. A. Mäder and A. Zunger, Effects of atomic clustering on the optical properties of III-V alloys, *Appl. Phys. Lett.* **64**, 2882 (1994).
- [33] J. Wu, W. Walukiewicz, K. M. Yu, J. W. Ager, E. E. Haller, H. Lu, and W. J. Schaff, Small band gap bowing in $\text{In}_{1-x}\text{Ga}_x\text{N}$ alloys, *Appl. Phys. Lett.* **80**, 4741 (2002).
- [34] G. Franssen, I. Gorczyca, T. Suski, A. Kamińska, J. Pereiro, E. Muz, E. Iliopoulos, A. Georgakilas, S. B. Che, Y. Ishitani, A. Yoshikawa, N. E. Christensen, and A. Svane, Bowing of the band gap pressure coefficient in $\text{In}_x\text{Ga}_{1-x}\text{N}$ alloys, *J. Appl. Phys.* **103**, 033514 (2008).
- [35] M. Moret, B. Gil, S. Ruffenach, O. Briot, C. Giesen, M. Heuken, S. Rushworth, T. Leese, and M. Succi, Optical, structural investigations and band-gap bowing parameter of GaInN alloys, *J. Cryst. Growth* **311**, 2795 (2009), proceedings of the 2nd International Symposium on Growth of III Nitrides.
- [36] See the Supplemental Material at <http://link.aps.org/supplemental/10.1103/PhysRevApplied.12.014055> for the analysis of the indium distribution within the samples and the description of the clustering-induced carrier localization and translational symmetry breaking.
- [37] R. Butté, L. Lahourcade, T. K. Uždavinyš, G. Callsen, M. Mensi, M. Glauser, G. Roszbach, D. Martin, J.-F. Carlin, S. Marcinkevičius, and N. Grandjean, Optical absorption edge broadening in thick InGaN layers: Random alloy atomic disorder and growth mode induced fluctuations, *Appl. Phys. Lett.* **112**, 032106 (2018).
- [38] M. Auf der Maur, B. Galler, I. Pietzonka, M. Strassburg, H. Lugauer, and A. Di Carlo, Trap-assisted tunneling in InGaN/GaN single-quantum-well light-emitting diodes, *Appl. Phys. Lett.* **105**, 133504 (2014).
- [39] L. Rigutti, L. Mancini, D. Hernández-Maldonado, W. Lefebvre, E. Giraud, R. Butté, J. F. Carlin, N. Grandjean, D. Blavette, and F. Vurpillot, Statistical correction of atom probe tomography data of semiconductor alloys combined with optical spectroscopy: The case of $\text{Al}_{0.25}\text{Ga}_{0.75}\text{N}$, *J. Appl. Phys.* **119**, 105704 (2016).
- [40] P. K. Basu, *Theory of Optical Processes in Semiconductors: Bulk and Microstructures* (Clarendon press, Oxford, 1997), Vol. 4.
- [41] M. J. Galtrey, R. A. Oliver, M. J. Kappers, C. J. Humphreys, P. H. Clifton, D. Larson, D. W. Saxey, and A. Cerezo, Three-dimensional atom probe analysis of green- and blue-emitting $\text{In}_x\text{Ga}_{1-x}\text{N}/\text{GaN}$ multiple quantum well structures, *J. Appl. Phys.* **104**, 013524 (2008).
- [42] C.-K. Tan, W. Sun, J. J. Wierer Jr., and N. Tansu, Effect of interface roughness on auger recombination in semiconductor quantum wells, *AIP Adv.* **7**, 035212 (2017).
- [43] M. Baranowski, Ł. Janicki, M. Gladysiewicz, M. Wełna, M. Latkowska, J. Misiewicz, Ł. Marona, D. Schiavon, P. Perlin, and R. Kudrawiec, Direct evidence of photoluminescence broadening enhancement by local electric field fluctuations in polar InGaN/GaN quantum wells, *Jpn. J. Appl. Phys.* **57**, 020305 (2018).